ELSEVIER

Journal of Atmospheric and Solar-Terrestrial Physics 66 (2004) 1615–1626

Journal of ATMOSPHERIC AND SOLAR-TERRESTRIAL PHYSICS

www.elsevier.com/locate/jastp

Statistical characteristics of VHF radar observations of low latitude *E*-region field-aligned irregularities over Gadanki

A.K. Patra*, S. Sripathi , V. Sivakumar, P.B. Rao[1]

National MST Radar Facility, Tirupati 517502, India

Available online 3 September 2004

Abstract

The statistical characteristics of *E*-region field-aligned irregularities observed with the Gadanki MST radar are presented and compared with observations made with the Piura radar at a similar magnetic latitude. Echoes are observed day and night, with the nighttime echoes being more intense and covering a greater height extent than during the day. The most probable echo occurrence times are just after sunrise (95%) and just before sunset (80%), when the echoing regions were centered around 95 and 100 km, respectively. The lowest probability of echo occurrence is found to be during noontime hours. The spectra of these echoes over Gadanki were all type 2. The mean Doppler velocities for altitudes above 105 km were upward at typically 10 m s^{-1} during the day and downward at about 10 m s^{-1} during the night. Spectral widths of 10–40 m s^{-1} were found during the day and 30–60 m s^{-1} during the night. These characteristics of *E*-region irregularities over Gadanki are quite similar to those found over Piura, and are remarkably different from those at either equatorial or higher latitudes.

1. Introduction

Extensive studies of *E*-region field-aligned irregularities (FAI) have been made in the equatorial and auroral regions with radars and in situ measurements (e.g., Kelley, 1989). In the last decade, intensive efforts have been made in both observation and theory to better understand FAI at midlatitudes (e.g., Fukao et al., 1998; Larsen, 2000). Special emphasis has been paid to understanding the so-called 'quasi-periodic' (QP) echoes. These echoes were first observed by Yamamoto et al. (1991) using the Middle and Upper atmosphere (MU) radar at Shigaraki, Japan and subsequently by many others (e.g., Kelley et al., 1995; Hysell and Burcham, 1999; Tsunoda et al., 1999; Haldoupis et al., 2001). A number of studies have also been made from the anomaly crest zone using the Chung-Li VHF radar (e.g., Pan et al., 1994; Huang et al., 1995; Chu and Wang, 1997; Huang and Chu, 1998; Pan and Tsunoda, 1998, 1999; Pan and Larsen, 2000).

At low latitudes, but outside the equatorial electrojet (EEJ) region, there have been very limited studies. These studies were made using the MST radar located at Gadanki (13.5°N, 79.2°E, dip 12.5°N), India (Choudhary et al., 1996; KrishnaMurthy et al., 1998; Choudhary and Mahajan, 1999; Patra and Rao, 1999; Pan and Rao, 2002; Patra et al., 2002a, b; Raghavarao et al., 2002) and the Piura VHF radar (5.2°S, 80.6°W, dip 13.9°N) in Peru (Woodman et al., 1999; Chau and Woodman, 1999; Chau et al., 2002). The above studies revealed that the characteristics of the low-latitude *E*-region FAI resemble, in some respects, those at midlatitudes and, in other respects, those from the equatorial electrojet. The observations revealed QP echoes (Chau and Woodman, 1999; Choudhary and Mahajan, 1999), large-scale

*Corresponding author.
E-mail address: patra_nmrf@rediffmail.com (A.K. Patra).
[1]Now at National Remote Sensing Agency, Balanagar, Hyderabad, India.

1364-6826/$ - see front matter
doi:10.1016/j.jastp.2004.07.032

gradient-drift waves (Patra and Rao, 1999; Patra et al., 2002a), and intermediate layer irregularities (Patra et al., 2002b). Detailed characterization and an understanding of the above aspects, however, are yet to emerge.

Radar spectral studies of *E*-region irregularities have shown mainly two types of irregularities, namely, types 1 and 2 (Kelley, 1989). Type-1 spectra have mean Doppler velocities close to the speed of ion acoustic waves (~360 m s^{-1}) and spectral widths much narrower than their mean Doppler velocities. Type-2 radar spectra are characterized by low mean Doppler velocities (much smaller than ion acoustic speed) and fairly broad spectral width. The mean Doppler velocities of type-2 spectra correspond to the line-of-sight electron drift velocity (Farley, 1985). Other types of spectra, namely types 3 and 4, have also been observed but only in auroral electrojets (for details, see Kelley, 1989).

For the equatorial and auroral electrojets, type-1 echoes are attributed to a modified two-stream instability and type-2 echoes to the gradient-drift instability. Due to the success of theoretical works in explaining the observations of equatorial and auroral electrojets, a similar line of approach has been adopted for other latitudes as well. However, the direct application of these instabilities at non-equatorial and non-polar latitudes is not so straightforward because the magnetic field lines are inclined and the zero-order electric fields are smaller. Woodman et al. (1991) pointed out this problem for midlatitudes and used the properties of gravity waves to reorganize the plasma in a way that satisfies the geometry for excitation of gradient-drift instabilities as the explanation for the occurrence of QP echoes. An alternate proposal based on the wind and wind shear (Kagan and Kelley, 1998) claims to avoid the problem associated with the electric field-driven process. In the context of these studies, the characteristics provided by our measurements of *E*-region FAI in low latitudes just outside the EEJ should be extremely valuable. This is so because at low latitudes the driving agents for the excitation of instabilities (such as the vertical electric field) is less, compared to the EEJ, and the blanketing *Es* is less frequent as compared to midlatitudes (e.g., Knecht and McDuffie, 1962). In addition, these studies could be used to improve the forecasting of equatorial spread-*F* irregularities since the *F*-region magnetic field lines over the dip equator map into *E*-region heights at low latitudes (Chau et al., 2002). Finally, according to Woodman et al. (1999), these irregularities could also be used as part of wireless communication systems. In fact, it is possible to communicate over distances of the order of 600–1000 km (Woodman, 1993). From this point of view our backscatter studies would be useful for the design of such communication systems.

The observations of *E*-region FAI from Gadanki so far have only been reported episodically without any particular occurrence statistics. On the other hand, good statistical studies (Woodman et al., 1999; Chau et al., 2002) from the Piura radar have already been published. Given the similar dip angles of the two locations (Gadanki and Piura) but different geographic latitudes (Gadanki located north and Piura located south of the geographic equator), it is highly desirable to make a study similar to that made from Piura and make a detailed comparison. In this paper, we present statistical results of *E*-region FAI observations gathered during 1994–2000. We also compare and discuss these results in detail with those made from Piura and other neighboring latitudes.

2. Experimental set-up

The observations reported here on low-latitude *E*-region irregularities were made using the mesosphere–stratosphere–troposphere (MST) radar located at Gadanki (Rao et al., 1995). The radar, while designed primarily for MST applications, was also intended for coherent backscatter study of ionospheric irregularities. Accordingly, the orthogonal phased-antenna arrays are aligned along the geomagnetic north–south and geomagnetic east–west directions (geomagnetic north is 2° west of geographic north). For the observations of *E*-region FAI, the antenna beam was positioned at a zenith angle of 13.2° (due magnetic north), which satisfies the field perpendicularity condition for *E*-region coherent backscatter. Thus, the radar detects the waves propagating perpendicular to the magnetic field in the magnetic meridian plane. The radar specifications and other important parameters used for the experiments are given in Table 1.

Table 1
Radar specifications and important parameters used for the *E*-region experiments

Parameter	Value
Frequency	53 MHz
Transmitter peak power	2.5 MW
Antenna	1024 3-element Yagi
Antenna area	12000 m^2
Beam width (one-way half power)	3°
Beam direction	13.2° off zenith and due north
Receiver gain	120 dB
Receiver bandwidth	1.7 MHz
Receiver dynamic range	70 dB
Pulse width	4 μs[a]
Inter-pulse period	1 ms[a]
Number of coherent integration	4
Number of FFT points	128

[a]On some occasions, the pulse width and inter-pulse period were 8 μs and 2 ms, respectively.

3. Observations

We have been operating the radar to study ionospheric FAI since its installation in 1993. Here, we present echo occurrence statistics for *E*-region FAI obtained from observations made during 1994–2000. Hundred and ninety five observational periods include 37 daytime, 146 nighttime, and 12 diurnal cycles. All observations were made between April and August (corresponding to spring and summer). Data were collected in the power spectral form and stored for post-analysis. Later, spectral characteristics were parameterized in terms of signal-to-noise ratio (SNR), mean Doppler velocity, and spectral width following the expressions given by Woodman (1985). SNR was computed using the noise power reckoned over the coherent integration filter bandwidth of 250 Hz (on some occasions, 125 Hz). We could detect signals with SNR as low as -12 dB (SNR of -12 dB for these data corresponds to ~0 dB detectability). Since meteor echoes could contaminate our *E*-region observations, consistency checks as a function of time based on the short-lived lifetimes of the meteor echoes allowed them to be removed.

Figs. 1a–c present the height-time variations of SNR, Doppler velocity, and spectral width corresponding to the diurnal cycle observed on July 15–16, 1998. Here, spectral width refers to the half-power full width of the Doppler power spectrum. The height and time resolutions of these observations are 600 m and 15 s, respectively. The horizontal bar at the bottom of each figure represents a data gap. It can be seen from Fig. 1a that the echoing region is confined to altitudes below 100 km during the daytime and seems to be structured in the form of two layers at the beginning of the run. In this case, these layers are found to have thicknesses of 2–3 km and are found to descend as time progresses. The echoes could be seen at altitudes as low as 87 km. Such layers are very common at Gadanki. Immediately after sunset, echoes started appearing at higher altitudes. Three echoing regions can be seen; one below 100 km, one just above 100 km and another at about 110–115 km. The two layers above 100 km also are found to descend, but at a relatively faster rate than during daytime. The topmost echoing region looks patchy and/or quasi-periodic in their occurrence and could be categorized as QP. Towards the end of the run (during 6–9 LT), the echoing region is very intense and confined to below 100 km. From this example, it appears that the echoes below 100 km are rather uniform, whereas above 100 km, they tend to be more structured.

The Doppler velocities (shown in Fig. 1b) are found to be mostly within $\pm 20\,\mathrm{m\,s^{-1}}$. Positive (negative) velocities correspond to velocities away from (towards) the radar. The velocities during daytime are found to be dominantly away from the radar till ~13 LT and towards the radar afterwards. During the night, the velocities can be either towards or away from the radar, and they change their directions more frequently than during the day. Furthermore, there seems to be a velocity altitude reversal. Similar observations were reported by Choudhary and Mahajan (1999), which were found to be associated with the QP echoes. The vertical wavelengths associated with the QP echoes observed by them were shown to be on the order of 18–20 km.

The spectral widths (shown in Fig. 1c) are found to be as high as $100\,\mathrm{m\,s^{-1}}$ or more, corresponding to the nighttime QP echoes and early morning intense echoes. During daytime, for similar echo strength, however, the spectral widths are much less ($\sim 50\,\mathrm{m\,s^{-1}}$) as compared to that of nighttime.

In Fig. 2, we present the percentage of *E*-region echo occurrence as function of local time and height. The continuous line represents the peak percentage of echo occurrence as a function of the time of day. We used 36 observational runs (12 daytime runs, 12 nighttime runs, and 12 diurnal cycles) to generate this figure. A threshold of -6 dB SNR (about 6 dB higher than the detectable limit of -12 dB) was used in generating this figure. The height and time bins in this figure are 1.2 km and 15 min, respectively. It may be noted that the echoes have extended to altitudes as high as 140 km (or more) and as low as 87 km. As the time progresses from midnight towards noon, the maximum altitude of significant echoes decreases from 120 km to less than 100 km and then rises after 16 LT. The higher altitude echoes, however, display patchy signatures. It can be noted that the peak percentage of signal occurrence during daytime and nighttime is found to be as high as 95% and 75%, respectively. The most probable times for echoes were found to be just after sunrise (95%), just before sunset (80%), and least likely around noon (<30%). The heights most likely to produce echoes were around 105 km from midnight to sunrise, 95 km right after sunrise, 100 km at sunset, and 90 km for a few hours after sunset. The variability of *E*-region FAI in the evening period may be useful for the prediction of spread *F* and, in fact, Chau et al. (2002) have shown that the likelihood of *F*-region irregularities over Piura and, therefore, topside spread *F* over Jicamarca is greater when there are no *E*-region irregularities over Piura. Further, around this time the pre-reversal enhancement of the vertical plasma drift (due to zonal electric field) takes place.

Figs. 3a and b present normalized occurrence probability distributions of SNR (left panel), velocity (middle panel), and spectral width (right panel) as a function of height corresponding to daytime and nighttime, respectively. Note that the range of daytime and nighttime SNRs is similar, with values as high as 36 dB (about 48 dB above the detectability level). Mean Doppler velocities during the day rarely exceed $\pm 50\,\mathrm{m\,s^{-1}}$,

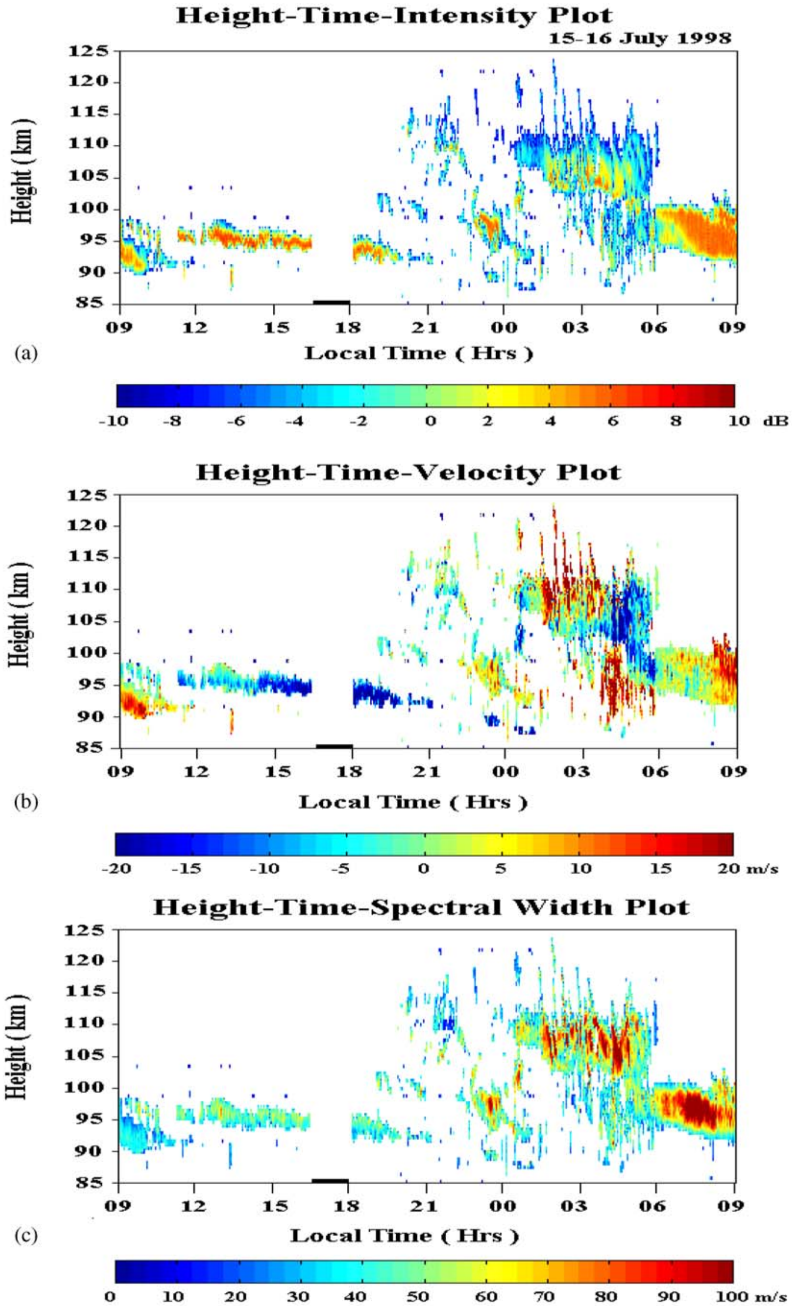

Fig. 1. Height–time plots of: (a) signal intensity (SNR in dB), (b) Doppler velocity, and (c) spectral width observed during a diurnal cycle observed on July 15–16, 1998.

whereas velocities above $\pm 50\,\mathrm{m\,s^{-1}}$ are common during the night. The mean values of the velocity distributions are close to zero in the lower altitudes (<105 km) during both day and night. At higher altitudes (>105 km), they are found to be $\sim 10\,\mathrm{m\,s^{-1}}$ away from the radar during the day and $\sim 10\,\mathrm{m\,s^{-1}}$ towards the radar during the night. Most spectral widths are found to be less than $60\,\mathrm{m\,s^{-1}}$ during the day, and 20–30 $\mathrm{m\,s^{-1}}$ higher during the night. The mean values of spectral width distributions corresponding to daytime and nighttime are in the

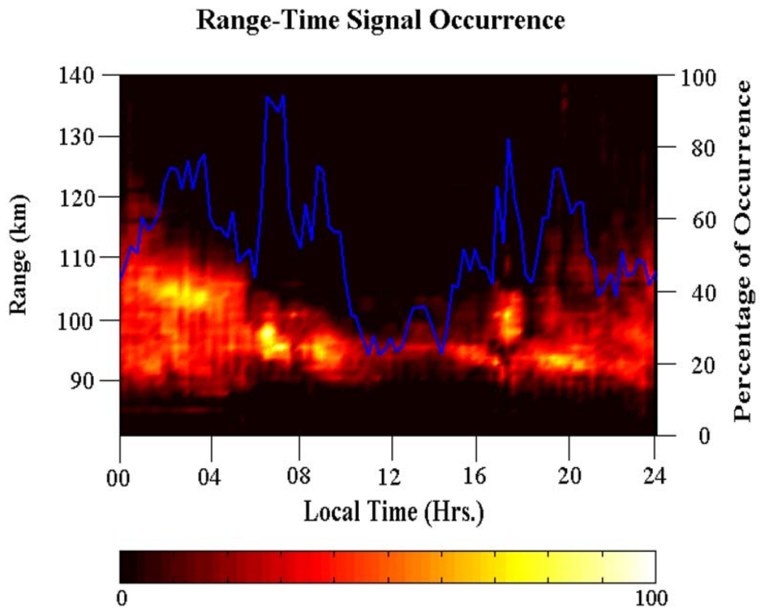

Fig. 2. (a) Height–time distribution of percentage of occurrence of the *E*-region echoes with a minimum of −6 dB SNR level. The continuous line represents the peak percentage of signal occurrence as a function of the time of day.

range 10–40 and 30–60 m s^{-1}, respectively. Spectral widths of echoes from 100 to 110 km are greater than those from lower altitudes.

Fig. 4 shows the diurnal variations of SNR (left panel), velocity (middle panel), and spectral width (right panel) in the form of scatter plots. No times are devoid of echoes, although the lower probability of echoes during the day above 105 km is evident. The velocities are found to be less variable during the day as compared to the night. Nighttime velocities vary more at higher altitudes than at lower ones. We believe that this higher variability is due to the polarization electric field associated with large-scale gradient drift waves and/or QP echoes. The spectral widths are quite similar for day and night at altitudes less than 95 km. At higher altitudes, the spectral widths are found to increase from their daytime values at about 18 LT, reach a maximum value at about 2 LT, and then decrease to their daytime values at about 6 LT.

In Figs. 5a and b we present the relation between SNR and spectral width as function of height for daytime and nighttime echoes, respectively. During the day, there are not many signals at higher altitudes and the relationships look similar. But during the night, the relationship suggests that irregularities at lower altitudes are not as turbulent as they are for the upper altitudes. Even for narrow spectra with widths as low as 25 m s^{-1}, the SNR can be as high as 30 dB. At higher altitudes the widths can be high, even for weaker echoes, essentially representing much more inhomogeneity and a greater degree of turbulence as compared to that of lower altitudes. In a turbulent medium, signal strength is expected to be proportional to the turbulent intensity represented by spectral width. Hence, the observations suggest that the medium is, in general, turbulent. Figs. 6a and b show the relationship between velocity and SNR for daytime and nighttime conditions, respectively. For the gradient drift instability associated with the EEJ, the Doppler velocity corresponds to the line-of-sight electron drift velocity, and the scattering cross section (which can be represented by SNR) is proportional to square of the drift velocity of electrons (Farley, 1985). In these figures, however, no such relationship can be noticed. SNR is found to be at maximum, even when the Doppler velocity is zero. For both daytime and nighttime, the range of values is about the same except that, during the nighttime, larger values of the Doppler shift are more probable.

The characteristics of the *E*-region FAI over Gadanki, including the ones reported earlier, can be summarized as follows:

1. The irregularities occur both during day and night. These irregularities become weaker (and sometimes disappear) during noon hours and extend to much higher altitudes during nighttime as compared to daytime (KrishnaMurthy et al., 1998).
2. The irregularities are field-aligned, i.e., they are detected only when the radar beam is perpendicular to magnetic field lines.
3. The echoing region can be categorized as thin, continuous layered structures at lower altitudes (at

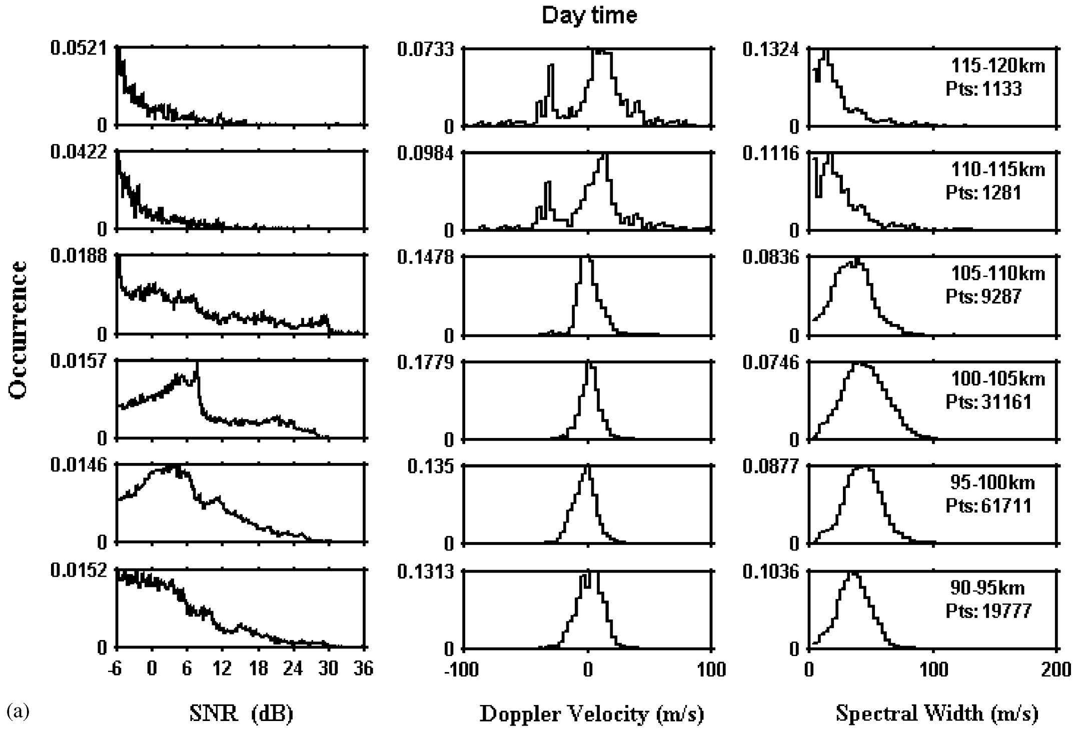

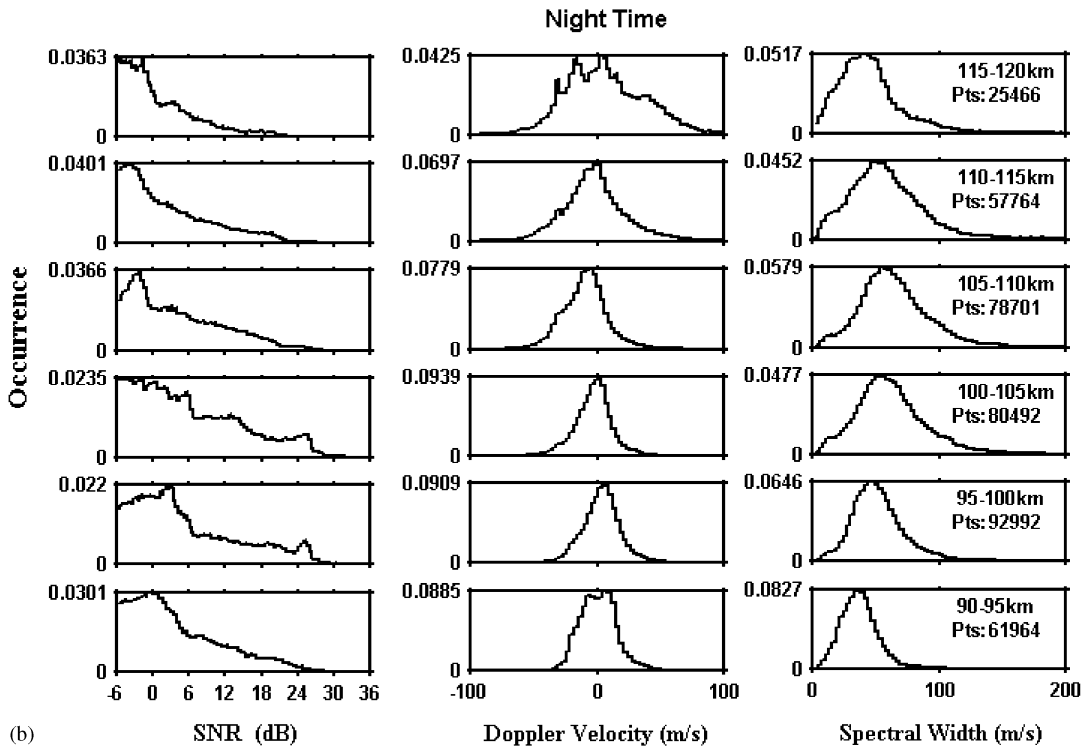

Fig. 3. (a) Normalized occurrence probability distributions of SNR (left panel), Doppler velocity (middle panel), and spectral width (right panel) corresponding to daytime hours (6–18 LT). The occurrence frequency is normalized to the number of data points mentioned in each panel. (b) Same as Fig. 3a, but for nighttime hours (18–6 LT).

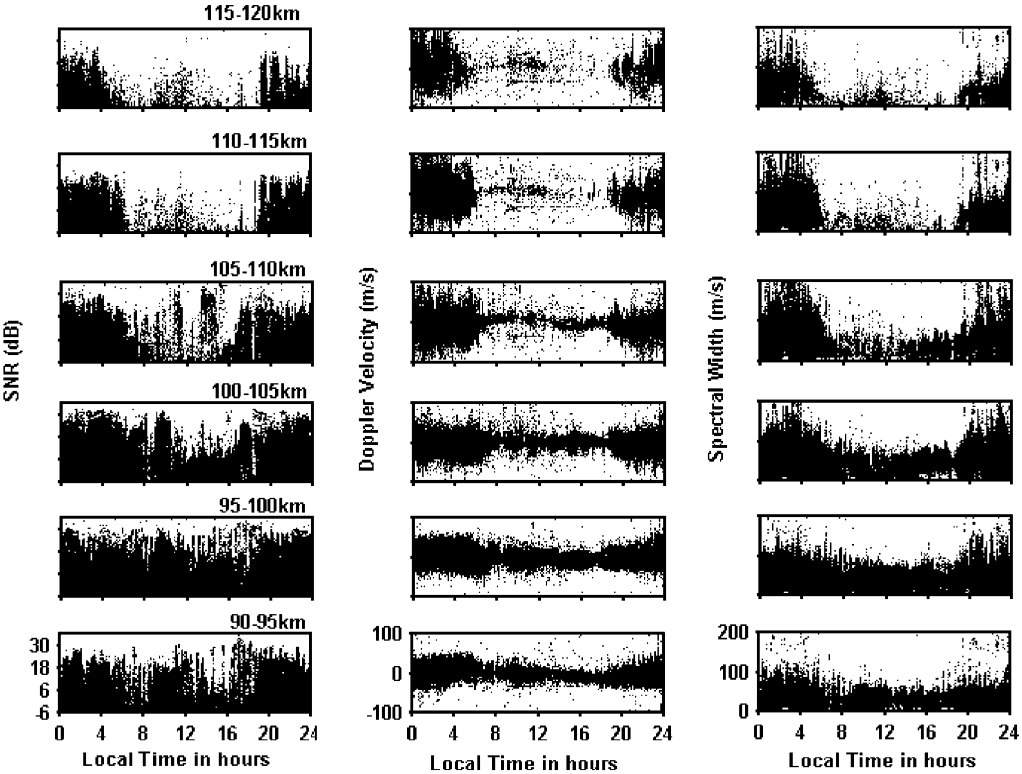

Fig. 4. Diurnal variations of SNR (left panel), Doppler velocity (middle panel), and spectral width (right panel) in the form of scatter plots.

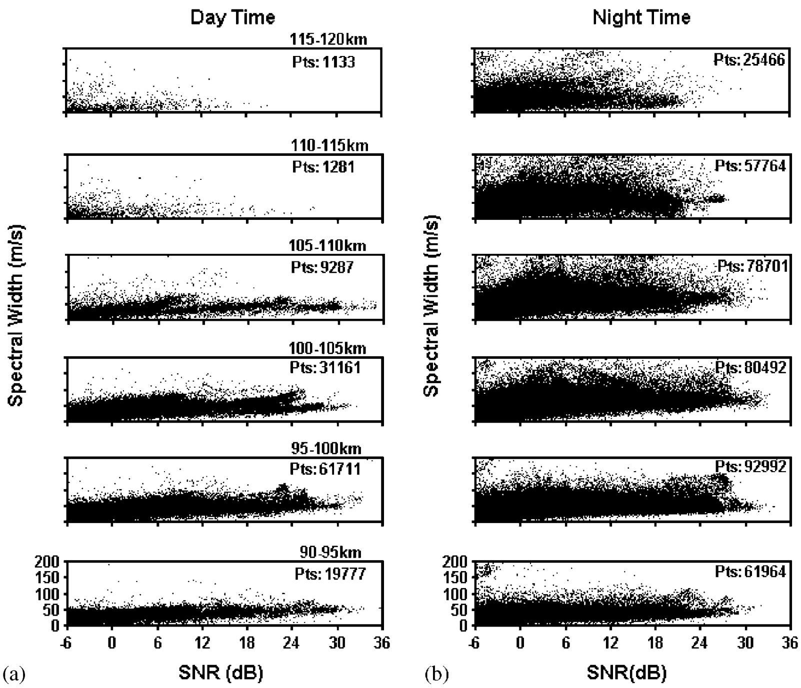

Fig. 5. Correlation between spectral width and SNR for: (a) daytime (6–18 LT) and, (b) nighttime (18–6 LT). 24 daytime and 24 nighttime observational runs are used. The number of data points is mentioned in each panel.

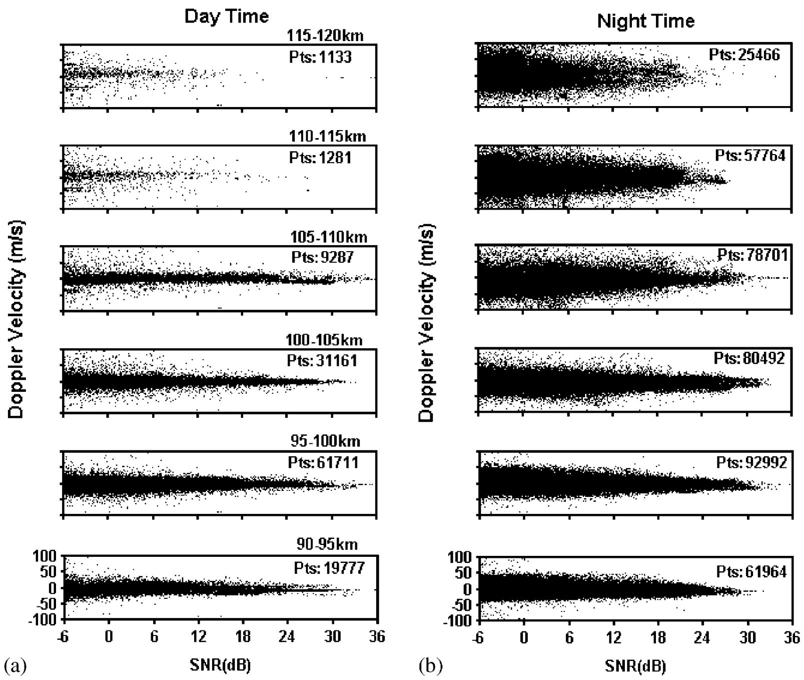

Fig. 6. Same as Fig. 5 but for Doppler velocity and SNR for: (a) daytime, and (b) nighttime.

or below 105 km) and thick patchy structures above. The echoing regions are found to descend as a function of time. The nighttime echoing regions, however, descend at higher rates than during daytime.

4. Kilometer-scale wave structures are observed at higher altitudes (Patra and Rao, 1999). The layers, which we mentioned earlier as being continuous, also show kilometer-scale wave structures at times (Pan and Rao, 2002; Patra et al., 2002a).
5. The nighttime echoes at higher altitudes show quasi-periodic structures quite similar to midlatitudes. The echoes also show the simultaneous occurrence of continuous echoes at lower altitudes and QP echoes at higher altitudes during nighttime (Choudhary and Mahajan, 1999).
6. On some occasions, the irregularities are found to extend to altitudes as high as 160 km (Patra et al., 2002b).
7. The spectral characteristics of the echoes are exclusively type 2 in nature.
8. The Doppler velocities corresponding to higher altitudes ($> \sim$105 km) are found to be generally upward during daytime and downward during nighttime (KrishnaMurthy et al., 1998). The Doppler velocities for lower altitudes, however, do not have a preferential direction and the mean values of the distributions are close to zero.
9. The vertical wavelengths observed in the Doppler velocity associated with QP echoes are of the order of 20 km.

4. Discussion

First, we compare the *E*-region FAI characteristics observed at Gadanki with those of Piura, reported by Woodman et al. (1999) and Chau et al. (2002). The observations from Piura, however, are confined to mainly nighttime. They observed that *E*-region echoes are stronger and occur more frequently during local summer (Chau et al., 2002). They observed mainly two echoing layers: one below 105 km (lower *E* region) and the other between 105 and 120 km (upper *E* region). On some occasions, they observed a descending third layer occurring between the two layers around midnight. Such layers have been seen at Gadanki around sunset, much earlier than those observed over Piura. At Gadanki, the upper *E*-region echoes, on some occasions, have been found to extend to altitudes as high as 160 km (Patra et al., 2002b). These echoes have been classified as intermediate layer echoes due to the characteristics of the echoing region resembling midlatitude intermediate layers (e.g., Mathews, 1998). The occurrence probabilities of the upper *E*-region echoes appear quite similar at both locations except that, on some occasions, this layer is observed up to 160 km in altitude (Patra et al., 2002b). These high altitude echoes occur less frequently and the SNR associated with these echoes are about 12 dB less than for echoes below 120 km (Patra et al., 2002b).

SNR observed by the Piura radar were found to be as high as 40 dB (Chau et al., 2002), which appear to be somewhat higher than that of Gadanki when the sensitivities of the two systems are normalized. The power-aperture product of the Piura radar is about 20 dB less sensitive than that of Gadanki (for a comparison, see Table 2). The SNR observed here, however, are comparable to nighttime EEJ type-2 signal strength (Fejer et al., 1975). The daytime values of SNR associated with the EEJ irregularities, however, are stronger than the nighttime values. The Piura radar detects *E*-region signals mostly between 18 and 8 LT and occasionally during the day (Chau et al., 2002). The Gadanki observations also show a tendency for signals to weaken or disappear during noontime. Hence, the general behavior of FAI observed at Gadanki and Piura is similar and both are remarkably different from that of EEJ. The daytime echo strength (except for noontime) at Gadanki, however, is quite similar to that of nighttime. That the Piura radar detected few echoes during daytime has been attributed to the low sensitivity of the Piura radar as compared to the Gadanki MST radar by Chau et al. (2002). However, given that the signal strength at Gadanki reaches 30 dB (about 42 dB above the detectability level) and given the sensitivity of the Piura radar (~20 dB lower than Gadanki radar), the Piura radar should detect signals during daytime if a similar signal strength is prevalent in the *E* region over Piura. Based on additional statistics, we feel that this lack of signal detection is not just due to the lower sensitivity of the Piura radar relative to that of Gadanki, but to different ionospheric conditions over the two sites as well. The observations suggest that the velocities are much less than the ion acoustic velocity. Even the maximum mean Doppler velocity added to the maximum spectral width does not reach 360 m s^{-1}, a condition required for the two-stream instability. Hence, *E*-region echoes over Gadanki are similar to type-2 echoes found in the EEJ but with smaller spectral widths. While the spectral widths of the EEJ 3-m irregularities often exceed 300 m s^{-1} (e.g., Balsley, 1969), the Doppler velocities observed at Piura corresponding to nighttime irregularities are within ±100 m s^{-1} and most of these are even within ±30 m s^{-1} (Woodman et al., 1999).The mean nighttime radial velocities corresponding to lower and higher echoes have been reported to be close to zero and ~7 m s^{-1} towards the radar, respectively. Hence for the nighttime echoes at both the places, the velocities are similar. The observations of daytime upward and nighttime downward velocities at higher altitudes are consistent with electrodynamic drift due to the daytime eastward and nighttime westward electric field. KrishnaMurthy et al. (1998) interpreted the higher altitude (>101 km) and lower altitude (<97 km) Doppler velocities as due to the equatorial *F*-region electric field and meridional neutral wind, respectively. Spectral widths measured by the Piura radar are found to be less than 150 m s^{-1} with their mean values in the range 60–75 m s^{-1} (Woodman et al., 1999; Chau et al., 2002), similar to those observed at Gadanki, indicating similar turbulent flow fields at the two locations.

Table 2
A sensitivity comparison of the Piura and Gadanki radars

Parameter	Value	
	Gadanki	Piura
Transmitter peak power	2.5 MW	20 KW
Antenna area	12000 m^2	10000 m^2
Duty cycle ratio	0.4%	0.66%

Comparing our observations with those of Piura and neighboring latitudes suggests that the Gadanki and Piura observations are similar in nature except for minor details (to be discussed later) and that both differ from those of the EEJ as well at midlatitudes. To date, our observations are too incomplete to study the seasonal characteristics as was done for Piura by Chau et al. (2002). This aspect will be studied in the future through additional experiments currently underway. Although the irregularities look quite similar to type-2 echoes of the EEJ or midlatitude sporadic *E*, they differ in detail. For example, EEJ echoes are stronger during daytime than at nighttime. The low-latitude echoes are weaker, in general, during daytime as compared to nighttime, whereas midlatitude echoes occur only during nighttime in association with sporadic-*E* layers. Type-1 echoes are a common feature in the EEJ because of the presence of large electric fields. Type-1 echoes have been observed at midlatitudes as well, but they are mostly isolated events (e.g., Schlegel and Haldoupis, 1994). Further, type-1 echoes have also been reported from the equatorial anomaly region using the Chung-Li VHF radar (Huang and Chu, 1998). However, type-1 echoes have not been observed thus far at either Gadanki or Piura. Since electric fields as large as ~15 mV/m are required to excite type-1 echoes at midlatitudes, Haldoupis et al. (1996) proposed a plausible two-dimensional model to account for the generation of large electric fields. They assumed an *E*-layer with sharp boundaries in the zonal direction and assumed a northward electric field, which then drives the plasma zonally. This in turn sets up a strong westward polarization electric field which may be 10 times larger than the ambient electric field and which produces an intense southward electron drift that is more than enough to excite the two-stream instability.

The fact that these echoes have not been observed at the low latitudes of Gadanki and Piura suggests that the ionospheric *E* region over these low latitude stations is much more homogeneous in the zonal direction than at midlatitudes and, accordingly, setting up large electric fields is more difficult. Also, the finite inclination of the magnetic field does not support a polarization field large enough to excite type-1 echoes.

An important difference between the Gadanki and Piura observations is the daytime occurrence of signals at Gadanki but not at Piura. From a sensitivity point of view, it seems that Piura should detect these echoes provided the conditions in the *E* region, and hence, the FAI strength over Piura, are similar to that at Gadanki. But the observations do not seem to support this viewpoint. KrishnaMurthy et al. (1998) have examined the growth rate of the gradient drift instability for the *E* region over Gadanki. They have shown that, for expected values of the electron drifts, the normal value of *E*-region electron density gradients is not sufficient to grow type-2 irregularities. Accordingly, they concluded that for smaller electron flow velocities (applicable for low latitudes), steeper gradients would be necessary. They hypothesized that the steep electron density gradients are generated by wind shear (gravity waves). During daytime the ionization production is quite significant, which plays an important role in the altitude profiles of electron density. Accordingly, the formation of such steep structures may be impeded due to the smoothing effect of production. They interpreted the disappearance or weakening of the echoes during noon hours (10–14 LT) as being due to the lack of steep electron density gradients at those times. They mentioned, however, that if the vertical wind shears are very strong, they could lead to the formation of blanketing *Es* and provide the necessary conditions for type-2 irregularities to occur, even during 10–14 LT.

Raghavarao et al. (2002) suggested that the variability of off-EEJ signals over Gadanki or similar latitudes during daytime is due to the electrodynamical effects of vertical shears in the zonal winds. They showed that during daytime, an eastward wind increasing with altitude, called a positive wind shear, produces whorls of westward currents and downward vertical electric fields that inhibit the development of gradient drift instability, whereas the wind shears of negative polarity engender whorls of eastward currents and upward electric fields, thereby enhancing the development of gradient drift instability.

We know that the EEJ is stronger over the South American sector than over the Indian sector (Viswanathan et al., 1992; Hari and KrishnaMurthy, 1995). Hence, the background **E** field may be larger over Piura than over Gadanki. Accordingly, for similar gradients in the electron density profile, we should expect signals to be observed over Piura. Perhaps the lack of echoes over Piura during the daytime can be attributed to the electrodynamical effects of wind and wind shear, that is, perhaps the wind pattern at *E*-region altitudes over the South American sector modifies the current system in such a way that it inhibits the growth of irregularities during daytime over Piura, but not always over Gadanki. Further study is needed on this issue.

5. Concluding remarks

We have found that many general characteristics of the irregularities observed at Gadanki and Piura are quite similar. There is, however, a significant difference in the occurrence probabilities of the irregularities during daytime. This aspect is yet to be understood. We see peaks in the percentage of echo occurrence just after sunrise and before sunset. We wish to study the sunset time characteristics in greater detail to find practical applications for spread-*F* prediction. Experiments to study the seasonal characteristics of these echoes are underway. The Doppler velocities corresponding to lower altitudes (<97 km) and higher altitudes (>102 km) could be used to estimate meridional neutral winds and equatorial *F*-region electric fields, respectively. Low latitude *E*-region FAI differ from those of the EEJ and midlatitudes in at least two counts: (1) the temporal behavior is significantly different (EEJ echoes are stronger during daytime than during nighttime whereas midlatitude echoes are basically a nighttime phenomena) and (2) the spectral characteristics above Gadanki are type 2 only (versus having both types 1 and 2 from the EEJ and midlatitudes).

Acknowledgements

The National MST Radar Facility (NMRF) is operated as an autonomous facility under the Department of Space with partial support from the Council of Scientific and Industrial Research. The authors are grateful to the NMRF technical staff, whose dedicated efforts enabled the observations reported here, and thank the referees for their valuable suggestions for improving the paper.

References

Balsley, B.B., 1969. Some characteristics of non-two-stream irregularities in the equatorial electrojet. Journal of Geophysical Research 74, 2333–2347.

Chau, J.L., Woodman, R.F., 1999. Low-latitude quasiperiodic echoes observed with the Piura VHF radar in the *E* region. Geophysical Research Letters 26, 2167–2170.

Chau, J.L., Woodman, R.F., Flores, L.A., 2002. Statistical characteristics of low latitude ionospheric field-aligned irregularities obtained with Piura VHF radar. Annales Geophysicae 20, 1203–1212.

Choudhary, R.K., Mahajan, K.K., 1999. Tropical *E*-region field-aligned irregularities: simultaneous observations of continuous and quasiperiodic echoes. Journal of Geophysical Research 104, 2613–2619.

Choudhary, R.K., Mahajan, K.K., Singh, S., Kumar, S., Anandan, V.K., 1996. First VHF radar observations of tropical latitude *E*-region field-aligned irregularities. Geophysical Research Letters 23, 3683–3686.

Chu, Y.H., Wang, C.Y., 1997. Interferometric observations of 3-dimensional spatial structure of sporadic *E* irregularities using Chung-Li VHF radar. Radio Science 32, 817–832.

Farley, D.T., 1985. Theory of equatorial electrojet plasma waves: new developments and current status. Journal of Atmospheric and Terrestrial Physics 47, 729–744.

Fejer, B.G., Farley, D.T., Balsley, B.B., Woodman, R.F., 1975. Vertical structure of the VHF backscattering region in the equatorial electrojet and the gradient drift instability. Journal of Geophysical Research 80, 1313–1324.

Fukao, S., Yamamoto, M., Tsunoda, R.T., Hayakawa, H., Mukai, T., 1998. The SEEK (Sporadic *E* Experiment over Kyushu) campaign. Geophysical Research Letters 25, 1761–1764.

Haldoupis, C., Schlegel, K., Farley, D.T., 1996. An explanation for the type-1 radar echoes from the mid-latitude *E*-region ionosphere. Geophysical Research Letters 23, 97–100.

Haldoupis, C., Hussey, G.C., Bourdillon, A., Dellone, J., 2001. Azimuth-time-intensity striations of quasi periodic radar echoes from the midlatitude *E*-region ionosphere. Geophysical Research Letters 28, 1933–1936.

Hari, S.S., KrishnaMurthy, B.V., 1995. Equatorial night-time *F*-region zonal electric field. Annales Geophysicae 13, 871–878.

Huang, C.M., Chu, Y.H., 1998. First observations of type-1 sporadic *E* irregularities in the equatorial anomaly region using the Chung-Li VHF radar. Geophysical Research Letters 25, 3779–3782.

Huang, C.M., Kudeki, E., Franke, S.J., Liu, C.H., Röttger, J., 1995. Brightness distribution of mid-latitude *E*-region echoes detected at the Chung-Li VHF radar. Journal of Geophysical Research 100, 14703–14715.

Hysell, D.L., Burcham, J.D., 1999. HF radar observations of quasi periodic *E* layer echoes over North America. Journal of Geophysical Research 104, 4361–4371.

Kagan, L.M., Kelley, M.C., 1998. A wind-driven gradient drift mechanism for midlatitude *E*-region ionospheric irregularities. Geophysical Research Letters 25, 4141–4144.

Kelley, M.C., 1989. The Earth's Ionosphere. Academic Press, San Diego, CA.

Kelley, M.C., Riggin, D., Pfaff, R.F., Swartz, W.E., Providakes, J.F., Huang, C.-S., 1995. Large amplitude quasiperiodic fluctuations associated with a mid-latitude sporadic *E* layer. Journal of Atmospheric and Terrestrial Physics 57, 1165–1178.

Knecht, R.W., McDuffie, R.E., 1962. On the width of the equatorial Es belt. In: Smith, E.R., Matsushita, S. (Eds.), Ionospheric Sporadic E. Pergamon Press, Oxford, pp. 215–218.

KrishnaMurthy, B.V., Ravindran, S., Viswanathan, K.S., Subbarao, K.S.V., Patra, A.K., Rao, P.B., 1998. Small-scale (~3 m) *E*-region irregularities at and off the magnetic equator. Journal of Geophysical Research 103, 20,761–20,772.

Larsen, M.F., 2000. A shear instability seeding mechanism for quasiperiodic radar echoes. Journal of Geophysical Research 105, 24931–24940.

Mathews, J.D., 1998. Sporadic *E*: current views and recent progress. Journal of Atmospheric and Terrestrial Physics 60, 413–435.

Pan, C.J., Larsen, M.F., 2000. Observations of QP radar echo structure consistent with neutral wind shear control of the initiation mechanism. Geophysical Research Letters 27, 867–870.

Pan, C.J., Rao, P.B., 2002. Low altitude quasi-periodic radar echoes observed by the Gadanki VHF radar. Geophysical Research Letters 29 25(1–4) doi:1025/2001GL014331.

Pan, C.J., Tsunoda, R.T., 1998. Quasi-periodic echoes observed with the Chung-Li VHF radar during the SEEK campaign. Geophysical Research Letters 25, 1809–1812.

Pan, C.J., Tsunoda, R.T., 1999. Semidiurnal behavior of quasi-periodic echoes in the mid-latitude Es region observed with the Chung-Li VHF radar. Geophysical Research Letters 26, 2621–2624.

Pan, C.J., Liu, C.H., Röttger, J., Su, S.Y., 1994. A three-dimensional study of *E*-region irregularity patches in the equatorial anomaly region using the Chung-Li VHF radar. Geophysical Research Letters 21, 1763–1766.

Patra, A.K., Rao, P.B., 1999. High resolution radar measurements of turbulent structure in the low-latitude *E*-region. Journal of Geophysical Research 104, 24667–24673.

Patra, A.K., Sripathi, S., Sivakumar, V., Rao, P.B., 2002a. Evidence of kilometer scale waves in the lower *E*-region using high resolution VHF radar over Gadanki. Geophysical Research Letters 29 137(1–4) doi:10.1029/2001GL013340.

Patra, A.K., Rao, P.B., Anandan, V.K., Jain, A.R., Viswanathan, G., 2002b. Evidence of intermediate layer characteristics in the Gadanki radar observations of the upper *E*-region field-aligned irregularities. Geophysical Research Letters 29 (14), 1696 doi:10.1029/2001GL013773.

Raghavarao, R., Patra, A.K., Sripathi, S., 2002. Equatorial *E*-region irregularities: a review of recent observations. Journal of Atmospheric and Solar-Terrestrial Physics 64, 1435–1443.

Rao, P.B., Jain, A.R., Kishore, K., Balamuralidhar, P., Damle, S.H., Viswanathan, G., 1995. Indian MST radar system 1, System description and sample wind measurements in ST mode. Radio Science 30, 1125–1138.

Schlegel, K., Haldoupis, C., 1994. Observations of the modified two-system instability in the midlatitude *E*-region ionosphere. Journal of Geophysical Research 99, 6219–6226.

Tsunoda, R.T., Burnocore, J.J., Saito, A., Krishimoto, Fukao, S., Yamamoto, Y., 1999. First observations of quasi periodic radar echoes from Stanford, California. Geophysical Research Letters 26, 995–998.

Viswanathan, K.S., Namboothiri, S.P., Rao, P.B., 1992. VHF and HF radar measurements of *E* and *F*-region plasma drifts at the magnetic equator. Journal of Geophysical Research 97, 3011–3017.

Woodman, R.F., 1985. Spectral moment estimation in MST radars. Radio Science 20, 1185–1195.

Woodman, R.F., 1993. Equatorial *E* and *F*-region scattering structures over Jicamarca. In: Hunsucker, R., Hunsucker, P. (Eds.), Trans-Equatorial and Near-Equatorial Radio Propagation Proceedings. Naval Postgraduate School, Monterey, CA.

Woodman, R.F., Yamamoto, M., Fukao, S., 1991. Gravity wave modulation of gradient drift instabilities in midlatitude sporadic *E* irregularities. Geophysical Research Letters 18, 1197–1200.

Woodman, R.F., Chau, J.L., Aquino, F., Rodriguez, R.R., Flores, L., 1999. Low latitude field-aligned irregularities observed in the *E* region with the Piura VHF radar: first results. Radio Science 34, 983–990.

Yamamoto, M., Fukao, S., Woodman, R.F., Ogawa, T., Tsuda, T., Kato, S., 1991. Midlatitude *E*-region field-aligned irregularities observed with the MU radar. Journal of Geophysical Research 96, 15943–15949.